Virtual-Ceiling-Line Following Robots and Its Mathematical Modeling

Apisak Worapishet

Mahanakorn Microelectronics Research Centre (MMRC)
MahanakornUniversity of Technology, Nongchok, Bangkok10530, Thailand
E-mail: apisak@mut.ac.th

Manuscript received November 21, 2016
Revised December 12, 2016.

ABSTRACT

A new robot guidance technique is introduced by making use of a virtual line connecting between the two adjacent ceiling marker points to guide the robot's movement. This so-called virtual-ceiling-line following robot offers lower installation and maintenance costs, as compared to its conventional floor-line following counterpart. In order to enable design investigation and possible optimization before an actual implementation, the mathematical models describing the robot's components that mainly control its movement are developed. These include the models for wheel movement, markers' position relative to the robot's position, and calculation of the alignment deviation. By utilizing the models in numerical simulations, the dynamic characteristics of the robot's movement are investigated. It is demonstrated that the models can be successfully employed for initial parameters adjustment of the PID controller before actual robot implementation.

Keywords: *Line-following robots, mathematical modeling, robot guidance, feedback control*

1. INTRODUCTION

The advent of automation and robotic technologies has helped transform the world into significantly more advanced society with unprecedented levels of accuracy and efficiency. Over the past few years, the deployment of robotics has rapidly expanded into a wide variety of industries ranging from aircraft to smart-phone manufacturing [1]. The robots have also increasingly been utilized in diversity of applications ranging from home cleaning to genetic drug discoveries [2].

One of the recent developments that symbolizes the transformative capability of robotic technologies, particularly in ecommerce, is the Amazon warehouse robots, where hundreds of goods-carrying robots are moving around the warehouse for automatic handling of on-line shopping orders [3]. The guidance of the so-called line-following robots relies upon a huge network of floor lines connecting thousands of stationary storing shelves. However, on the down side, the guidance technique entails a burdening cost for installing and maintaining the networks of lines covering a vast amount of area of a warehouse floor.

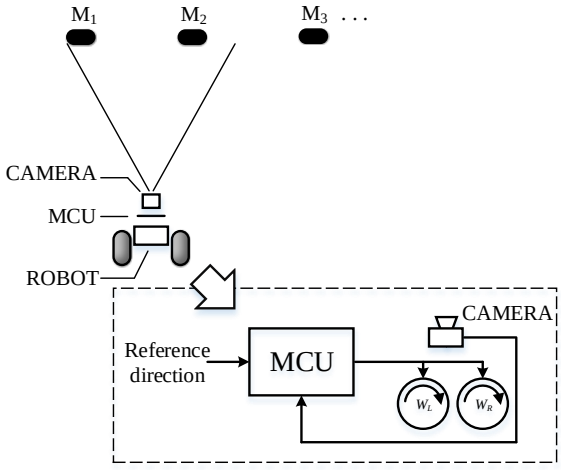

Fig.1 *Components and block diagram of the virtual-line following robot system. Reference direction is moving path of robot.*

It is thus the objective of this work to develop an alternative means to guide the robot movement. Instead of using lengthy marker lines on the warehouse floor, we make use of marker points installed intermittently on the ceiling. In this way, the robot is guided by the virtual line connecting two adjacent marker points, which can be a couple of meters apart thereby significantly

reducing the installation cost. In addition, the ceiling makers requires minimum maintenance because they have no contact with any moving robots, unlike the floor markers which are constantly in contact with passing robots' wheels, thereby eroding and making the lines faded over time.

The overview of the virtual-ceiling-line following robot system is outlined in Section 2. Also given in this section is the mathematical models for the system components. This is followed by numerical simulations in Section 3 and conclusion in Section 4.

2. VIRTUAL-LINE FOLLOWING ROBOT

2.1 System Overview

The block diagram of the virtual-line following robot system is shown in Fig. 1. It is essentially a feedback control system consisting of a robot, an installed camera pointing to ceiling, and a micro-controller unit. The camera is used to capture the image of two ceiling markers nearby the robot. The image is then processed by the micro-controller to identify the x-y pixels of the image that locate the marker points, typically of a circle shape. The virtual line connecting the two markers is then determined, and the alignment deviation between the virtual line's direction and the robot's moving path is calculated. This deviation is subsequently processed to determine the speed of the robot's left and right wheels in a way to turn the robot's moving direction to align with the virtual line. In this work, it is assumed that the distance between adjacent markers are selected such that only two markers are captured by the camera image at one time.

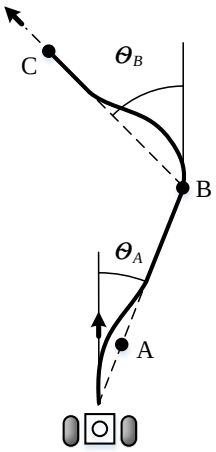

Fig. 2 *Virtual lines connecting ceiling markers and typical moving trajectory.*

Fig. 2 illustrates typical virtual lines connecting ceiling markers (dash lines) and moving trajectories (thick solid lines) where the robot initially adjusts its moving direction to align with the virtual line AB between the ceiling markers A and B. When the robot approaches the marker B, it eventually switches to adjust its direction to align with the virtual line BC, and so on. In this way, it can be seen that the robot can be guided from the starting location to the destination in a piece-wise virtual-line following manner.

2.2 Mathematical Modeling

In order to design and optimize the dynamic responses of the virtual-line following robot, it is critical to know the parameters and analytical equations describing the input/output transfer function associated with each block in the system of Fig. 1. In this way, a suitable PID controller can be designed accordingly. However, the transfer functions from the markers' locations to the alignment deviation can be both complicated and nonlinear. This makes it difficult to design the PID parameters in an analytical manner. As a result, one may have to resort to implementing an actual virtual-line following robot system so that the PID parameters can be adjusted until the desired response is achieved. However, such an empirical design methodology is time-consuming and so inefficient that it may not lead to design optimization.

To address this issue, the mathematical models for the virtual-line following robot system of Fig. 1 is developed. The models can be employed for numerical simulations of the whole system where all the parameters can be explored and efficiently designed to meet the desired response without any real implementation. It is necessary to develop a set of mathematical equations to calculate the successive co-ordinates and directions while the robot is moving, given the speeds of its right/left wheels and the time interval. Since the image captured by the installed camera on the moving robot continually changes, a set of equations modeling the movement of the maker points on the image are required, given the positions of the markers and the robots in the reference co-ordinate. Also required are the equations for calculating the deviation which is the essential feedback parameter for adjusting robot and virtual-line alignment. The transfer function of the PID controller implemented inside the micro-controller, MCU in Fig.1, is well-known and hence not included here. For the motor's response, it is of a first-order type. The details of the modeling equations are the subject of the following sub-sections.

2.3 Modeling of Moving Co-ordinate and Direction

We first start by formulating the movement of the robot from the reference co-ordinate at (x,y) = (0,0) and the reference direction set along the $+y$ axis, as shown in Fig. 3(a) and (b). The robot moves to the right (Fig. 3(a)) following a circular arc when the speed of the left wheel is higher than that of the right wheel, and vice versa (Fig. 3(b)) when the speed of the right wheel is higher. Since the left/right wheels share the same moving arc angle θ, the following relations between the angle, and the distances travel by the wheels can be given by

$$\theta r_L = v_L \Delta t, \tag{1a}$$

$$\theta r_R = v_R \Delta t. \tag{1b}$$

In the equations, w is the distance between the wheels, r_L and r_R are the arc radii, v_L and v_R are the speeds of the moving left/right wheels, and Δt is the time interval. Consider right-moving wheels in Fig. 3(a).By putting $r_L = r_R + w$, dividing (1b) by (1a) and then solving for r_R and r_L, we have

$$r_R = \gamma_v w/(1-\gamma_v), \tag{2a}$$

$$r_L = r_R + w. \tag{2b}$$

where $\gamma_v = v_R/v_L = r_R/(r_L + w)$. Putting (2a) into (1b), the moving arc angle is given by

$$\theta = +(1-\gamma_v) v_R \Delta t/\gamma_v w. \tag{2c}$$

It is assumed that the angle is positive in the clockwise (CW) or right-moving direction. Similarly, the equations for the left-moving wheels in Fig. 3(b) are given by

$$r_L = \gamma'_v w/(1-\gamma'_v), \tag{3a}$$

$$r_R = r_L + w, \tag{3b}$$

$$\theta = -(1-\gamma'_v) v_L \Delta t/\gamma'_v w, \tag{3c}$$

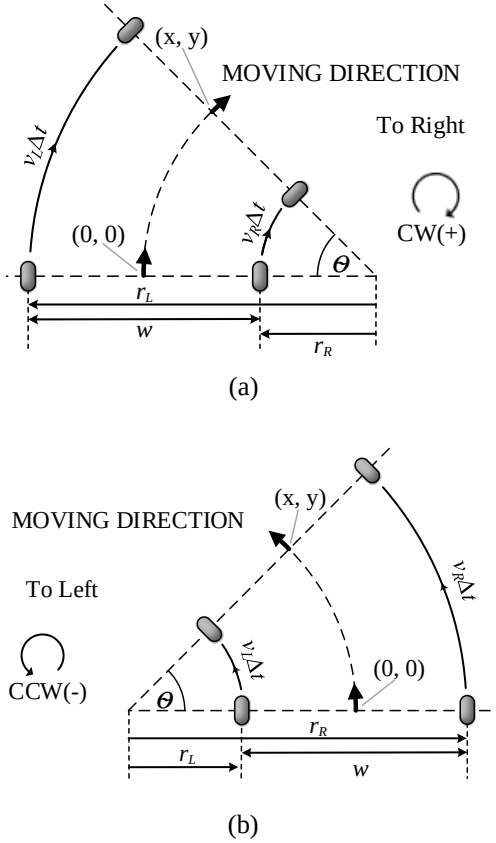

Fig. 3 *Geometric models for (a) right-moving wheels and (b) left-moving wheels.*

where $\gamma'_v = v_L/v_R = r_L/(r_R + w)$. Note that the angle is negative in the counter-clockwise (CCW) or left-moving direction. By using (2) and (3), the destination co-ordinate (x, y) and the direction angle (with reference to $+y$-axis) of the robots, for the starting co-ordinate at (0, 0), are as follows. For the right-moving direction, we have

$$\theta = +(1-\gamma_v) v_R \Delta t/\gamma_v w, \tag{4a}$$

$$y = (r_R + w/2) sin\theta, \tag{4b}$$

$$x = (r_R + w/2)(1 - cos\theta). \tag{4c}$$

For left-moving direction. We have

$$\theta = -(1 - \gamma'_v)v_L \Delta t/\gamma'_v w, \quad (5a)$$

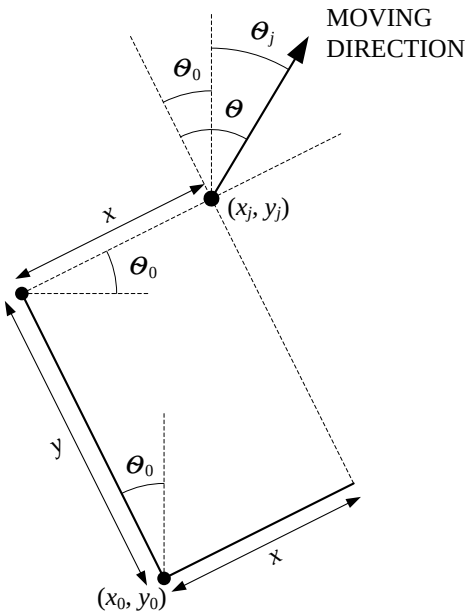

Fig.4 *Geometric model for calculation of destination coordinate starting from arbitrary co-ordinate.*

$$y = -(r_L + w/2)sin\theta, \quad (5b)$$

$$x = -(r_L + w/2)(1 - cos\theta). \quad (5c)$$

Fig. 4 shows the destination co-ordinate (x,y) for the case when the robot moves from an arbitrary co-ordinate at (x_0, y_0) and direction angle θ_0 from the +y axis. Based on the geometric relations in the figure, together with the sign definition of θ and the use of (4) and (5), we have

$$y_j = y + (y \cdot cos\theta_0 + x \cdot sin\theta_0)\,, \quad (6a)$$

$$x_j = x + (x \cdot cos\theta_0 - y \cdot sin\theta_0). \quad (6b)$$

For the moving direction at the destination co-ordinate (x, y), it is given by

$$\theta_j = \theta_0 + \theta \quad (6c)$$

2.4 Modeling of Ceiling Markers' Positions on Robot's Installed Camera Image

As the robot moves, the position of the marker on the video image captured by the installed camera will change accordingly. As suggested by Fig. 5, the relative position (x^c, y^c) of the ceiling marker is related to both the maker's position (x^m, y^m), and the current position

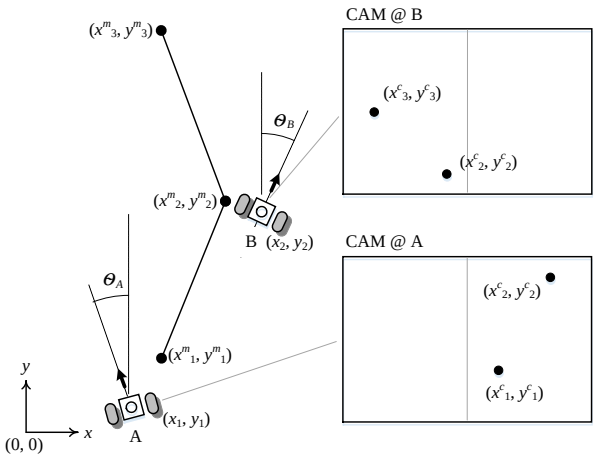

Fig. 5 *Captured Images by Robot's Camera* (*CAM*) *at different positions A and B.*

(x_j,y_j) and direction angle θ_j of the robot in the reference co-ordination frame. Thus, by calculating the translations along the x and y axes, followed by the angle rotation. we have

$$x_j^c = \Delta x \cdot cos\theta_j - \Delta y \cdot sin\theta_j, \quad (7a)$$

$$y_j^c = \Delta x \cdot sin\theta_j + \Delta y \cdot cos\theta_j, \quad (7b)$$

where

$$\Delta x = x^m - x_j, \quad (7c)$$

$$\Delta y = y^m - y_j. \quad (7d)$$

2.5 Calculation of Alignment Deviation

Having calculated the relative position of the markers on the captured image, we can now find the alignment deviation between the robot's current moving path and the virtual line connecting the markers. As also illustrated in Fig. 6, this may be quantified by extrapolating the virtual line to the top or bottom of the captured image. Subsequently, the deviation, D_v^T or D_v^B, can be determined from the image by calculating the distance between the top or bottom extrapolated points and the center vertical line, which is the reference line for the robot's moving path. Based on the geometric relations as indicated in Fig. 6, it can be shown that

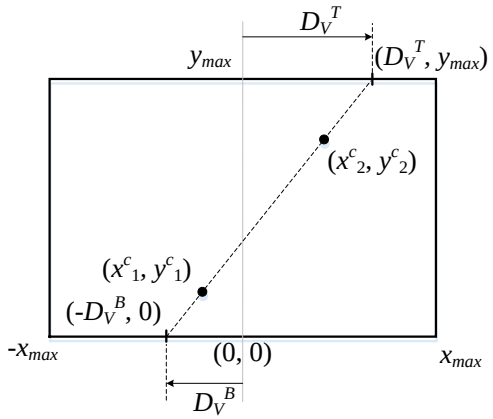

Fig. 6 *Definitions and geometric relations of deviation parameters, D_v^T and D_v^B.*

$$K = \frac{\Delta y}{\Delta x} = \frac{\Delta y_T}{\Delta x_T} = \frac{\Delta y_B}{\Delta x_B}, \qquad (8a)$$

where

$$\Delta x_T = D_v^T - x_2^c, \qquad (8c)$$

$$\Delta y_T = y_{max} - y_2^c, \qquad (8c)$$

$$\Delta x_B = x_1^c - D_v^B, \qquad (8d)$$

$$\Delta y_B = y_1^c. \qquad (8e)$$

By solving (8), we have

$$D_v^T = \frac{1}{K}(y_{max} - y_2^c) + x_2^c, \qquad (9a)$$

$$D_v^B = x_1^c - \frac{1}{K} y_1^c \quad . \qquad (9b)$$

The closed-loop feedback system of Fig.1 will try to minimize D_v^T or D_v^B, which, as a result, adjust the alignment of the virtual line and the moving direction of the robot.

3. NUMERICAL SIMULATIONS

In this section, numerical simulations based upon the developed mathematical models are demonstrated in order to investigate the moving dynamics of the virtual-line following robot. The parameters setup is as follows. For the robot, the wheel distance is w = 0.25 m, the nominal velocity of the left/right wheels is v = 1.0 m/sec, and the starting position is at the co-ordinate (0, 0). The motor's time constant is set at T_m = 100 msec. which is a typical value for the employed robot's motor.

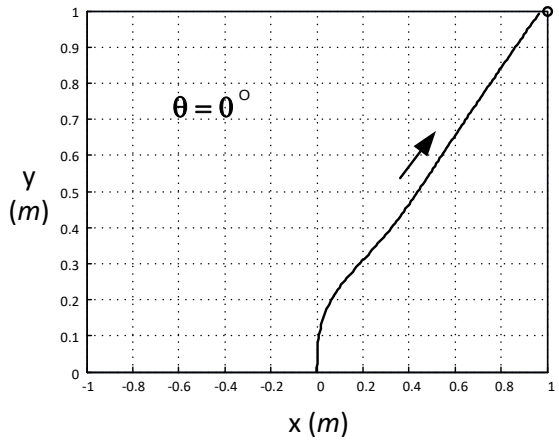

(a)

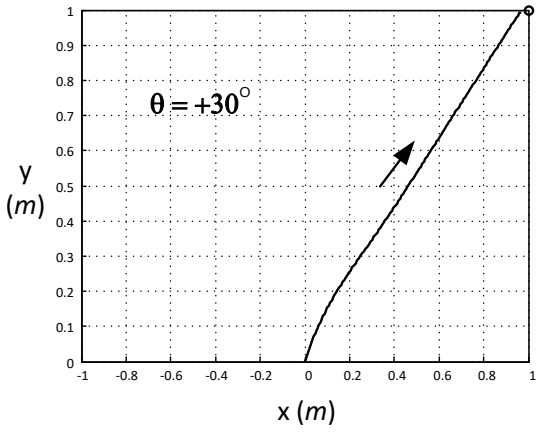

(b)

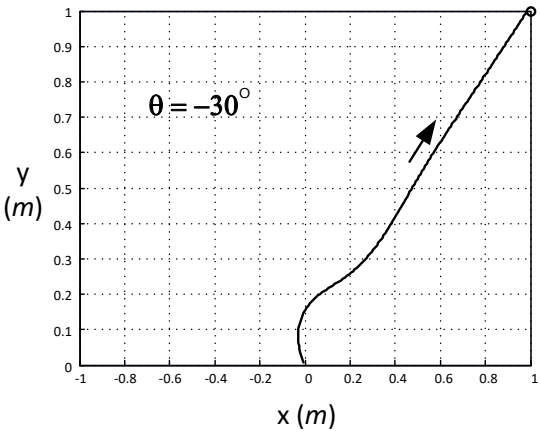

(c)

Fig. 7 *Simulated trajectories at different initial angles.*

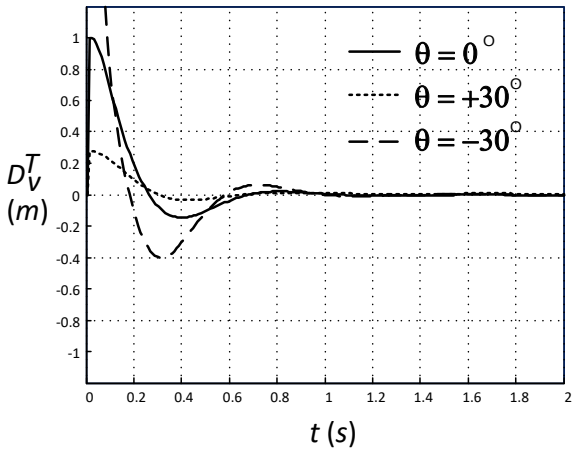

Fig. 8 *Simulated top deviation responses at different initial angles.*

For the installed camera, the maximum co-ordinates of the captured video image along the x-axis and y-axis are x_{max} = +1 m, y_{max} = +2.0 m [cf. Fig. 6]. The positions of the two markers are at the co-ordinate (+1, +1) and (+2, +2) in meter unit. The time step is set at Δt = 0.1 sec. D_v^T is chosen as the feedback parameter. By performing extensive parametric simulations, the proportional parameter of the PID controller are set at K_p = 0.1 (m/sec)/m, the integration parameter at K_I = 0.01 (rad/sec)-(m/sec)/m. The differentiation parameter is zero.

Fig. 7(a)-(c) show the simulation results for the moving trajectories on the reference co-ordination (x, y) versus time. The starting angles θ were at 0^o, $+30^o$, and -30^o which results in the angles of -45^o, -15^o, and -75^o from the virtual line connecting the two markers. As evident, the robot can adjust its moving direction to align with the virtual line at different initial angles. The responses of the alignment deviation versus time are given in Fig. 8 to show the dynamics of the moving trajectories. It is noticed from the figure that the robot's moving paths converge to align with the virtual-line with slight oscillatory responses. In addition, the plots show that the convergence time is (to less than 1% error) within 1.0 sec.

4. CONCLUSION

The virtual-ceiling-line robot guidance technique, which promises lower installation and maintenance costs, has been introduced. The mathematical models for dynamical simulations of the robot movement have been developed. Given a set of specific robot parameters, the models were successfully employed for initial parameter designs by virtue of parametric numerical simulations. The design indicates that the dynamical characteristic of the virtual-line following robot's movement is close to optimum critical responses and that the time required for alignment is less than 1.0 sec at the nominal robot's speed of 1.0 m/sec. Future works include actual robot implementation, and practical verification of the models.

REFERENCES

[1] "History of Industrial Robots," the International Federation of Robotics – IFR 2012.

[2] M. Anand, and S. Clarice, "*Role of Robot Scientists and Artificial Intelligence in Drug discovery*," International Journal Of Engineering and Computer Science, Volume 4, No. 3, March 2015, pp. 10668-10673.

[3] J. T. Li1, and H. J. Liu, "*Design Optimization of Amazon Robotics Automation*," Control and Intelligent Systems, Volume 4, No. 2, 2016, pp. 48-52.

[4] M. S. Islam and M. A. Rahman, "*Design and Fabrication of Line Follower Robot*," Asian Journal of Applied Science and Engineering, Volume 2, No. 2, 2013.

Apisak Worapishet received the B.Eng. degree (with first-class honors) from King Mongkut's Institute of Technology Ladkrabang, Bangkok, Thailand, in 1990, the M.Eng.Sc. degree from the University of New South Wales, Australia, in 1995, and the Ph.D. degree from Imperial College, London, U.K., in 2000, all in electrical engineering. Since 1990, he has been with Mahanakorn University of Technology, Bangkok, Thailand, where he currently serves as the Director of Mahanakorn Microelectronics Research Center (MMRC). He also serves as the Editor-In-Chief of the ECTI Transactions on EEC, and the Associate Editor of IEEE Transactions on Circuits and Systems – I, Regular Papers. His current research interest includes mixed-signal CMOS analog integrated circuits, Bio-medical sensors, wirelined and wireless RF CMOS circuits, microwave circuits, reconfigurable and embedded circuits and systems.